DOI 10.1007/s10517-018-4032-y
Cell Technologies in Biology and Medicine, No. 4, February, 2018

Analysis of the Basic Characteristics of Osteogenic and Chondrogenic Cell Lines Important for Tissue Engineering Implants

N. M. Astakhova[1,2], A. V. Korel'[1], E. I. Shchelkunova[1], K. E. Orishchenko[3], S. V. Nikolaev[3], U. S. Zubairova[3], and I. A. Kirilova[1]

Translated from *Kletochnye Tekhnologii v Biologii i Meditsine*, No. 4, pp. 249-257, October, 2017
Original article submitted May 24, 2017

We isolated and characterized cultures of bone and cartilage tissue cells of laboratory minipigs. The size and morphological features of adherent osteogenic and chondrogenic cells were specified. During long-term culturing under standard conditions, the studied cultures expressed specific markers that were detected by immunohistochemical staining: alkaline phosphatase and calcium deposits in osteoblasts and type II collagen and cartilage extracellular matrix in chondrogenic cells. Proliferative potential (mitotic index) of both cell types was 4.64% of the total cell number. Cell motility, *i.e.* the mean velocity of cell motion was 49 pixels/h for osteoblasts and 47 pixels/h for chondroblasts; the mean migration distance was 2045 and 2118 pixels for chondroblasts and osteoblasts, respectively. The obtained cell lines are now used as the control for evaluation of optimal biocompatibility of scaffold materials in various models. Characteristics of the motility of the bone and cartilage tissue cells can be used for modeling and estimation of the rate of cells population of 3D scaffolds made of synthetic and biological polymers with different internal structure and physicochemical properties during designing *in vitro* tissue implants.

Key Words: *osteogenic and chondrogenic cells; mitotic index; migration rate; 3D scaffold*

Osteoblast and chondroblast cultures are used for studying the biochemistry and physiology of bone and cartilage formation and molecular and cellular bases of various pathologies of the musculoskeletal system in humans. Osteoblast culture is also used for studying the mechanisms of bone resorption and formation; chondroblast cultures are employed for studying the formation and functioning of the cartilaginous tissue under normal and pathological conditions. In addition, these cultures are used for screening of potential anabolic agents and for the development and testing of new biomaterials and can serve as the cell source for tissue engineering.

The development of biosynthetic regenerative implants and tissue engineering are urgent problems of modern medicine. Tens of millions of injuries of the musculoskeletal system of different etiologies requiring surgical interventions occur every year around the world. In most cases, bone material or a substitute for reconstruction of large bone tissue defects is required. Taking into account aging of the population worldwide and growing frequency of bone injuries, the need for bone implants will undoubtedly increase in the future. Recent efforts of researchers were focused on designing and fabrication of 3D scaffolds that are more preferable substrate for cell proliferation. Tissue engineering with the use of cells, growth factors, and 3D scaffols as the carriers for cells is a modern clinical approach for regene-

[1]Ya. L. Tsivyan Novosibirsk Research Institute of Traumatology and Orthopedics, Ministry of Health of the Russian Federation; [2]Innovative Medical and Technology Center (Medical Technopark); [3]Federal Research Centre Institute of Cytology and Genetics, Siberian Division of the Russian Academy of Sciences, Novosibirsk, Russia. ***Address for correspondence:*** nastakhova@niito.ru. M. N. Astakhova

ration of extensive bone defects and correction of traumatic bone injuries.

The key strategy for bone defect repair is transplantation of scaffolds populated by mesenchymal stem cells and differentiated osteogenic cells. The development of spatial structures for correction of the bone defects with the use of 3D printing technology is in progress. Biopolymers and calcium phosphate compounds are used as the material for printing. This method allows obtaining precision constructs of intricate geometry and desired architectonics [2]. However, the osteoinductive and osteoconductive properties of these materials are insufficient for correction of gross defects (>1 cm^3) [2,16]. This is due to several factors: bone and cartilaginous tissue should endure mechanical stress and should have balanced elastic—strength characteristics. Too rigid implant (*e.g.*, metal—ceramic composite) can damage the surrounding tissues.

Another problem is weak adhesion properties of the scaffold surface for population by osteogenic cells. Extensive defects of the skull vault are replaced with composite polylactide scaffolds obtained by phase separation of poly-L-lactide, calcium glycerophosphate, and collagen gel. Calcium glycerophosphate modulates the osteoinductive properties of the scaffold, while collagen gel improves biocompatibility of polylactide [3,19]. This modification increases biocompatibility of the scaffold for cells [1]. Microfibrous polylactide matrices are characterized by high mechanical strength, are biodegradable, and exhibit no toxicity. However, due to the absence of polar functional groups, polylactide matrices are highly hydrophobic, which adversely affects adsorption of proteins and considerably limits cell migration deep into pores of the 3D structures (cell proliferation is observed only on the surface and in the adjacent layers). Thus, for optimization of the processes of infiltration and cell proliferation, modification the scaffold surface [14] and a special perfusion system for population of the matrices with cells are required [3].

For solving the problem of slow *in vivo* matrix population with cells, substances initiating bone regeneration are used. In case of large defects and appropriate size of the scaffolds, the deeper cells penetrate into the scaffold, the worse is microcirculation, which leads to poor supply with nutrients, slow transmission of humoral signals and cell response to them, *i.e.* deceleration of cell metabolism in the tissue engineering construct. Recent studies in this area showed that the use of mechanical, electrical, and electromagnetic stimuli [4,11] promoted differentiation and normal functioning of bone cells [13] and cartilaginous tissue cells [10] and accelerated population of 3D scaffolds by cells [5], but these factors are still underestimated during implant designing.

Thus, some problems in bone regeneration remain unsolved despite the diversity of scaffold materials and methods of their fabrication. There are no clear protocols of cell application and special equipment ensuring uniform population of the matrices with cells. There is no doubt that solution of these problems requires integrated interdisciplinary approach considering many factors.

Our aim was to study basic morphological and functional characteristics of bone and cartilaginous tissue cells: adhesion, cell size, mitotic index, and trajectory and mean velocity of cell migration on cultural plastics. These characteristics of cells are supposed to be used for modeling and calculation of the rate of population of 3D scaffolds by cells during designing of tissue implants *in vitro*.

MATERIALS AND METHODS

Experimental model. The study was performed on laboratory minipigs bred at the Institute of Cytology and Genetics for laboratory and preclinical studies. At the Ya. L. Tsivyan Novosibirsk Research Institute of Traumatology and Orthopedics, minipigs are used for modeling of the bone and cartilage defects and their correction by transplantation of tissue engineering constructs in *in vivo* experiments. The experiments were carried out in accordance with European Convention for the Protection of Vertebrate Animals used for Experimental and other Scientific Purposes and Order of the Ministry of Health of the Russian Federation (March 19, 2003).

Cell isolation and culturing. Chondrogenic cells were isolated from the cartilage tissue of the knee joint of 2 experimental female minipigs aging 1-1.5 weeks. Hyaline cartilage was washed for 15 min in Hanks' solution with kanamycin (1 g/liter), crushed to 0.5 mm^2 in a Petri dish with minimum volume of RPMI-1640, and then incubated in 1.5% collagenase solution for 5-8 h at 37°C on a shaker. The cell suspension was filtered through a Nylon filter and centrifuged 10 min at 1500 rpm. The obtained cell suspension was brought to a concentration of 3×10^5/ml with RPMI-1640 supplemented with 10% fetal calf serum (FCS; Gibco) and 100 U/ml penicillin and streptomycin (BioloT) and then incubated in plastic flasks (TPP) in a CO_2 incubator (37°C, 5% CO_2).

Cells expressing specific markers of osteoblasts, osteogenic lineage cells, were isolated from fragments of cancellous bone tissue of the femoral head. The conditions of culturing and stimulation of primary osteoblasts on plastic were chosen. To this end, several types of culture media DMEM GlutaMax, RPMI, and RPMI GlutaMax (Gibco) were tested. The combination of growth medium RPMI GlutaMax with 10%

FCS (Gibco) was optimal for long-term culturing of osteoblasts under standard conditions of CO_2 incubator (37°C and 5% CO_2). In cultures of both cell types, the medium was changed every 3-4 days. Confluent cultures of both types were harvested from plastic with 0.25% trypsin (Sigma) in 1 mM EDTA (1-3 min at 37°C) and precipitated by centrifugation at 1500 rpm for 5 min. Passage 5-15 cells were used in the experiments.

Morphometry and immunohistochenistry. In representative samples of primary osteoblasts and chondroblasts, the mean cell diameters were determined. Cell diameters were measured in the suspension in PBS after harvesting of the confluent monolayer with 0.25% trypsin. Morphometric measurements were carried out using AxioVision Le Rel 4.3 (Carl Zeiss) and Morpho Images software.

To confirm chondrogenic properties of the cultured cells, they were stained with antibodies to collagen II carrying a fluorescent label Alexa Fluor 568 (Invitrogen). This specific marker of chondrogenic differentiation is clearly seen in the cell cytoplasm (Fig. 1, *a*). The intensity of collagen II fluorescence in chondrocytes varied within the cell population. During long-term culturing, chondroblasts start to produce cartilaginous tissue matrix specifically stained with alcian blue. The intensity of alcian blue staining is proportional to the thickness of the cartilage matrix (Fig. 1, *b*).

Differentiation of osteoblasts *in vitro* can be characterized by three stages: cell proliferation, matrix maturation, and matrix mineralization.

During all stages, osteoblasts express specific proteins, markers of these cells that can be detected by immunohistochemical staining. Alkaline phosphatase is detected at the stage of cell proliferation and its expression reaches the maximum at the stage of matrix maturation. That is why this specific marker was chosen to determine the degree of osteoblasts differentiation. Measurement of alkaline phosphatase activity after reaction with the substrate BCIP/NBT (Amresco) was carried out visually. Depending on alkaline phosphatase activity, the cells were stained from slightly bluish to dark blue-violet (Fig. 1, *c*). Osteoblasts at the stage of mineralization produce numerous intercellular calcium deposits *in vitro*. This process attests to successful formation of the bone tissue. Calcium deposits can be specifically stained bright red with alizarin red S dye. In cell clusters, the intensity of red color is proportional to the intensity of mineralization (Fig. 1, *d*). Colored cells were analyzed under a AxioObserver Z1 light microscope (Carl Zeiss) using ZEN 2012 software (blue edition).

Cell-IQ analysis of the main characteristics of cells. Proliferative potential (mitotic index), migration trajectories, and motor activity of osteoblastic and chondroblastic cells were analyzed in two independent experiments cell by culturing in Cell-IQ long-term observation system for 4 days at 37°C; 5% humidified CO_2 was pumped directly through the culture plate in the following regimen: 15 min pump on, 15 min pump off, initial gas supply for 30 min. The cells were photographed over 43 h with a Nikon CFI Plan DL Fluorescence objective (×10), 6 times per hour, 3 fields per well of a 12-well plate, 3 wells for each cell line. The images were analyzed using Cell-IQ Analyser software. For calculation of the mitotic index in Cell-IQ Analyser, the total number of cells and the number of dividing cells were counted. A library of images for detection and recognition of flattened cells, dividing cells, and cellular debris was collected (Fig. 2, *a*, *b*).

On the basis of this library and selected parameters (minimum distance between neighbor cells, maximum cell diameter, cell symmetry, *etc*.), a protocol was created and all the images were analyzed. The mitotic index was calculated by the formula: MI=100%×M/N, where M and N are the number of dividing cells and the total number of cells, respectively, for each field of view over the entire period of observation. Motor activity was evaluated for 18 randomly selected cells by measuring the length of their trajectories over the entire observation period or until the cell left the field of view (Fig. 3, *a*-*c*).

Cell mobility on substrates with different rigidity (plastic and gelatin) was also analyzed in Cell-IQ system (Fig. 4). To this end, we chose cultures with low initial seeding density (~400 cells/cm^2). Cell tracking on the time-lapse images was performed manually using a Fiji image processing package (http://fiji.sc/Fiji). We analyzed trajectories of cells that did not contact with other cells over the period of tracking, *i.e*. trajectories that were determined by activity of these particular cells, but not their contacts with other cells and did not depend on the location of other cells. For calculation of the characteristics of cell mobility, special programs were developed using Mathematica 10 package.

RESULTS

Primary porcine osteoblast line was first isolated by the previously described methods [6,7] with modifications at the Ya. L. Tsivyan Novosibirsk Research Institute of Traumatology and Orthopedics for studying the basic characteristics of bone cells for bone implants designing and for biological assessment of substrates for scaffolds. Similar studies in Russia and abroad employ expensive commercial mouse preosteoblasts line MC3T3 and rat cells (DSMZ PromoCell GmbH) [8,9,20] or osteosarcoma cell lines MG63, TE85, and

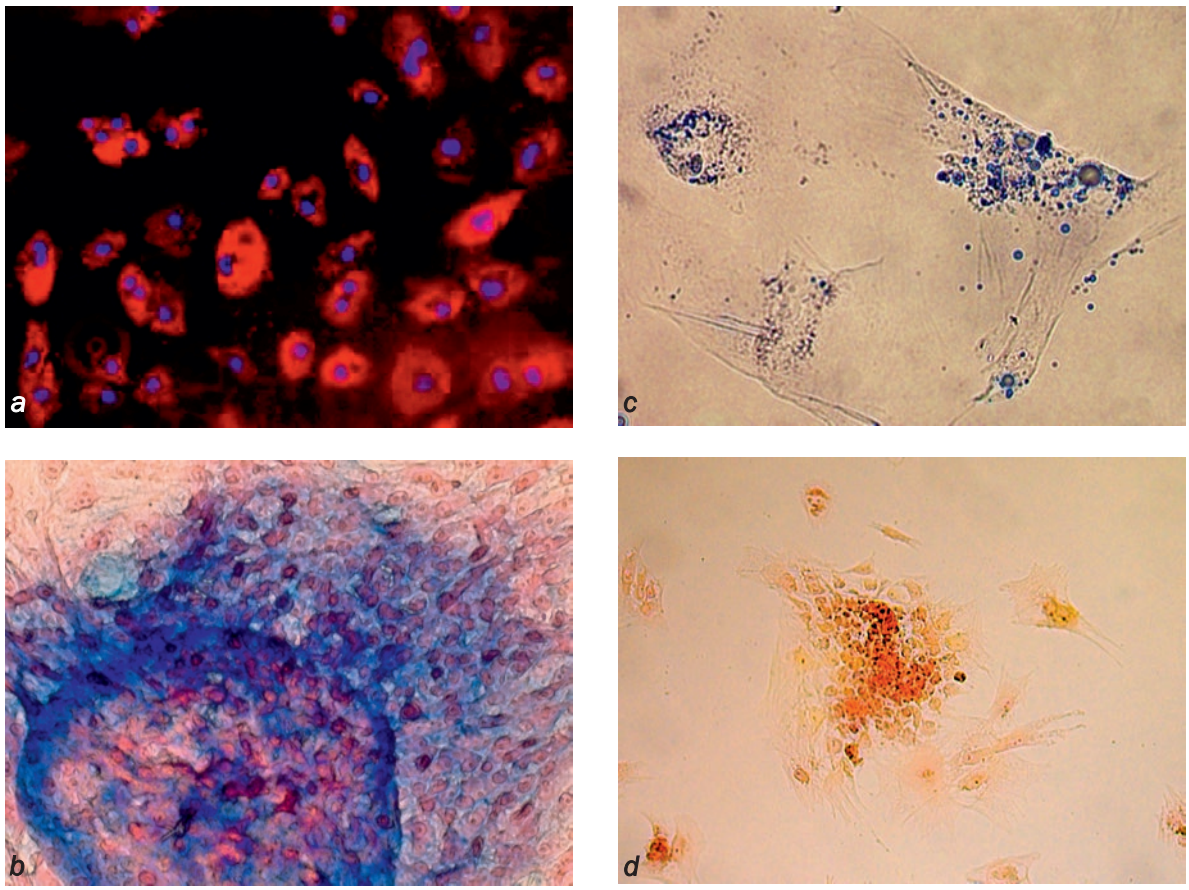

Fig. 1. Cytochemical markers of chondrogenic (*a*, *b*) and osteogenic (*c*, *d*) cells, ×20 (*a*, *d*), ×10 (*b*, *c*). *a*) Staining for collagen II, cell nuclei are stained with DAPI; *b*) alcian blue staining, cell nuclei are stained with Nuclear Fast Red; *c*) staining for alkaline phosphatase; *d*) staining alizarin red S.

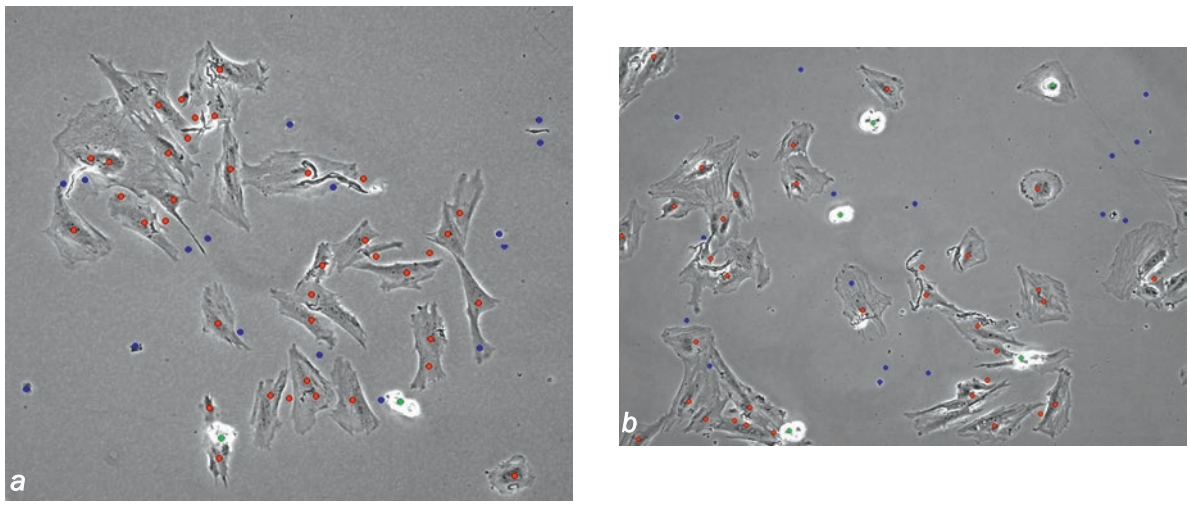

Fig. 2. Detection of flattened cells, dividing cells, and cell debris using Cell-IQ Analyser system. *a*) Primary osteoblasts; *b*) primary chondroblasts. Red dots: flattened cells, green dots: dividing cells, blue dots: cell debris.

SaOS2 that carry chromosome rearrangements potentially affecting their osteogenic properties [7].

Chondrogenic cells mostly represent slightly elongated cells with round large nucleus containing 1-2 nucleoli. Osteogenic lineage cells are larger, with greater cytoplasm and shorter and sharp processes; in mature osteoblasts, the cytoplasm contains linear structured microfilaments and medium-sized nuclei with 2-3 nu-

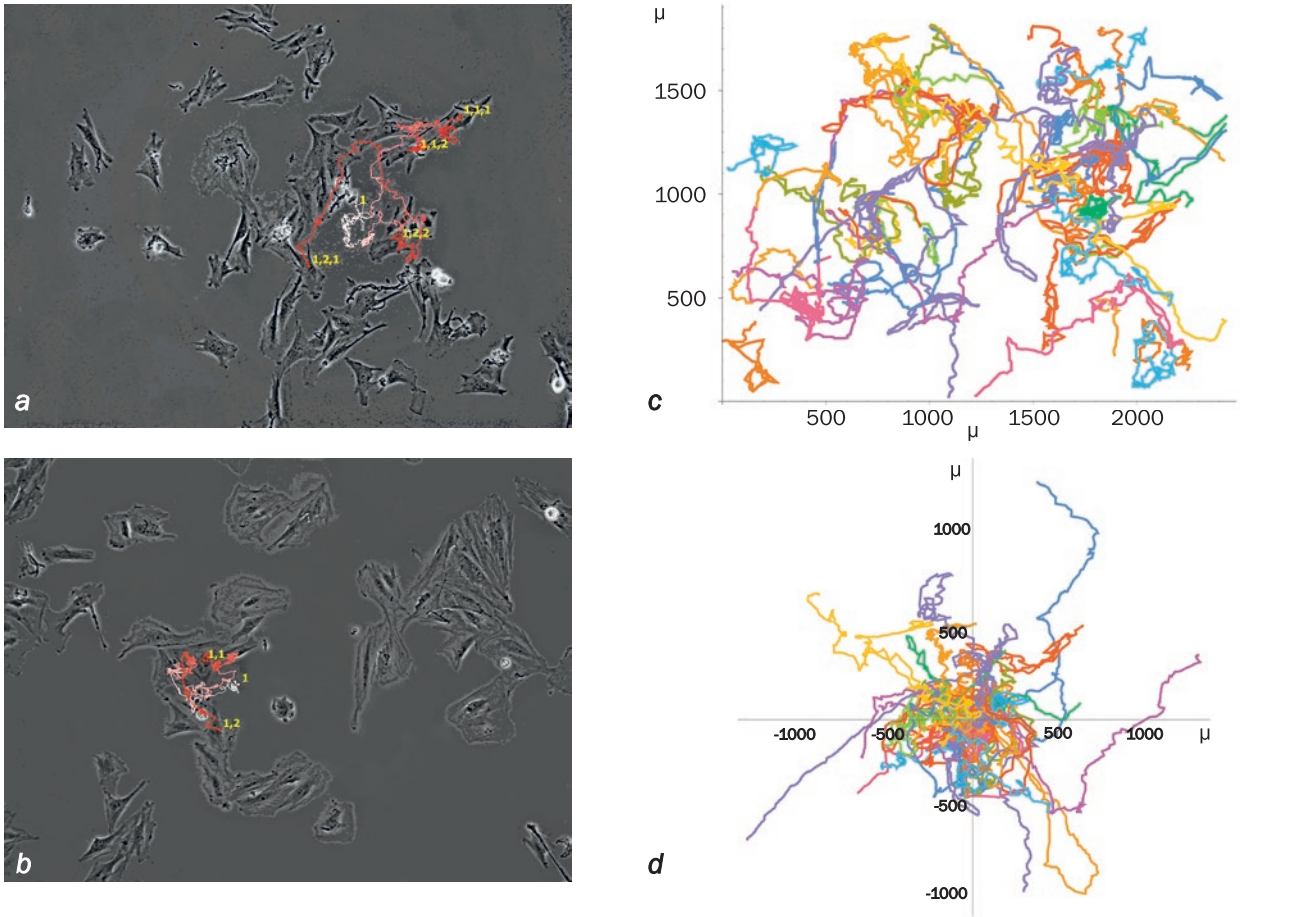

Fig. 3. Visualization of cell trajectories. *a*) Trajectory of a chondroblast and its descendants; *b*) trajectory of osteoblast and its descendants; *c*) summary graph (from 12 frames) of trajectories of chondroblasts in culture plastics; *d*) the same trajectories in a coordinate system tied to the beginning of each trajectory. Trajectories of different cells is shown in different colors.

cleoli. Morphometric analysis showed heterogeneity of populations of young, growing, and large mature cells in both osteoblast and chondroblast cultures. The diameter of chondrogenic cells varied from 12.97 to 26.70 μ (mean 16.75 μ; Table 1). The mean diameter of osteogenic cells was 17.37 μ, but this value varied in a significantly broader range (from 9.33 to 29.91 μ), which was consistent with previous reports on the size of bone cells; for instance, the diameter of mature osteoclasts can reach 150 μ and more [12]. Large size of differentiated cells of both types (up to 30 μ) should be taken into account when choosing the materials for scaffolds: materials with pore size of 250 μ or more are more preferable. In previous studies of infiltration, proliferation, and differentiation of osteoblasts on scaffolds, more intensive cell migration and infiltration were observed in scaffolds with larger pores [18].

Mitotic index was calculated for both cell types. For primary osteoblasts and primary chondroblasts, the mitotic index was 4.64% of the total number of cells, *i.e.* cell lines of both types actively proliferated and were characterized by similar potential, which was seen from the curves showing total cell number throughout the experiment (43 h) (Fig. 5, *a*, *b*).

Motor activity was evaluated for 9 randomly selected cells (one in each field) and all its descendants. To this end, the trajectory of a selected cell before division and then the trajectories of all its descendants were traced using Cell-IQ Analayser software (Fig. 3, *a*, *b*). As a result, we evaluated the mean velocity of cells of both types. The mean velocity of cell migration was 49 pixels/h for osteoblasts and 47 pixels/h for chondroblasts; the mean lengths of trajectories for chondroblasts and osteoblasts were 2045 and 2118 pixels, respectively, which allows considering them as actively moving cells (own observations).

The study of cell mobility and development of methods of its evaluation have a more than 100-year history. At the phenomenological level, cell mobility can be described in terms of Ornstein—Uhlenbeck (OU) model by the formula

$$<\vec{d}(t)2>=2nD(t\text{-}P(1\text{-}e\text{-}tP))$$

for the mean square cell displacement:

$$\vec{d}(t)=\vec{r}(t)\text{-}\vec{r}(0)$$

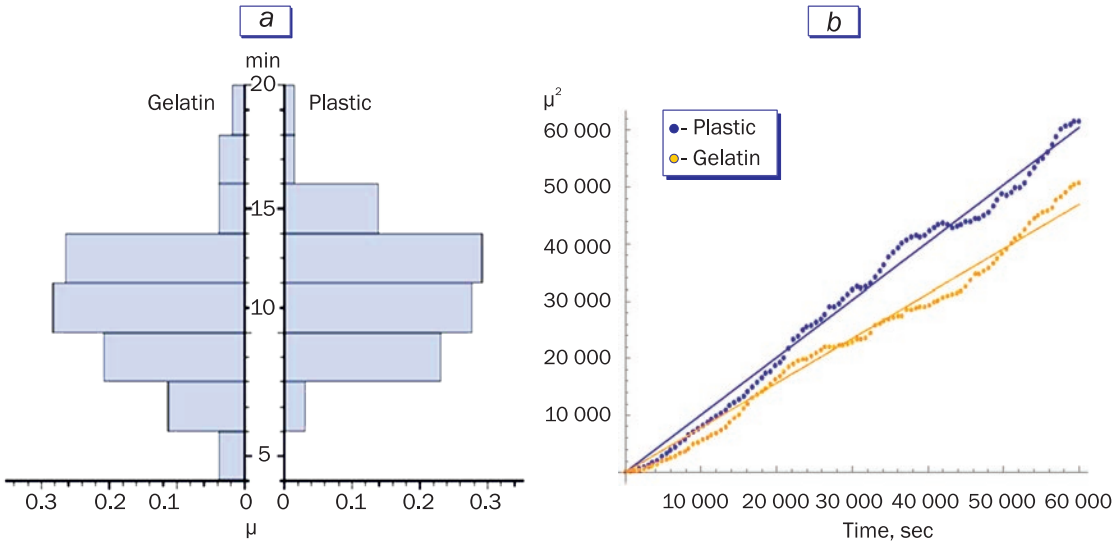

Fig. 4. Chondroblast mobility of the plastic and on gelatin substrate. *a*) Frequency distribution of chondroblast displacement lengths (μ per 10 min) on gelatin and plastic; *b*) mean square of cell displacement as a function of time on plastic and gelatin. Straight lines: approximation of experimental data within the framework of the Brownian motion model.

from the beginning of its trajectory; <...> is expected value; t is time; n=1, 2, 3 is dimension of the space where the trajectories $\vec{r}(t)$ are studied; D is the diffusion coefficient of the OU process and is referred to as the cell motility coefficient; P is the persistence time of the motion [15]. However, to begin with, the cell motility can be viewed in terms of the simple diffusion model. To this end, special programs for importing the data from the Fiji image processing package, formation of sets of tracks that meet certain criteria, their visualization (Fig. 3, *c*, *d*), computation of movement elements such as cell displacement, vectors of displacement, turning angles, and calculation of their statistics (Fig. 4, *a*), and calculation of the characteristics of cell mobility in terms of simple Brownian motion were created (Fig. 4, *b*).

Preliminary results showed that the stiffer is the surface, the higher was cell mobility, which is consistent with previous findings [17].

Lines of cartilaginous and bone tissue cells were obtained for further optimization of studies aimed at creation of *in vitro* model of tissue implants. In experiments on long-term culturing of chondroblasts and osteoblasts with visual control using the Cell-IQ system, the sizes and morphology of cells in heterogeneous populations were determined. Histochemical markers were selected to confirm chondrogenic and osteogenic nature of cells. The mobility of both cell types in Brownian motion approximation was evaluated. Mitotic index, the distance passed by an individual cell per time unit, the trajectory, and mean velocity the chondroblasts and osteoblasts during their long-term incubation on plastic were evaluated. Thus, the experimental methods and algorithms/software for information retrieval and interpretation developed in the course of our experiments allow us to characterize and modulate physicochemical conditions in the potential scaffold material intended for implants and cell reaction to these conditions. Selection of optimal conditions will help to develop standard protocols for obtaining individual cell 3D constructs for regenerative therapy.

The authors are grateful to E. V. Mamonova, General Director of Innovative Medical Technology Center (Medical Technopark) and S. I. Baiborodin, Head of the Microscopic Analysis of Biological Objects Common Use Centre, Federal Research Centre Institute of Cytology and Genetics, Siberian Division of the Russian Academy of Science.

The work was supported by the Russian Foundation for Basic Research (grant No. 15-29-04875);

TABLE 1. Diameter (μ) of Chondroblasts and Osteoblasts.

Cells	*n*	Min	Max	M	SEM	SD
Osteoblasts	27	9.33	29.91	17.37	1.01	5.26
Chondroblasts	27	12.36	26.70	16.75	0.57	2.98

Note. *n*: number of analyzed cells.

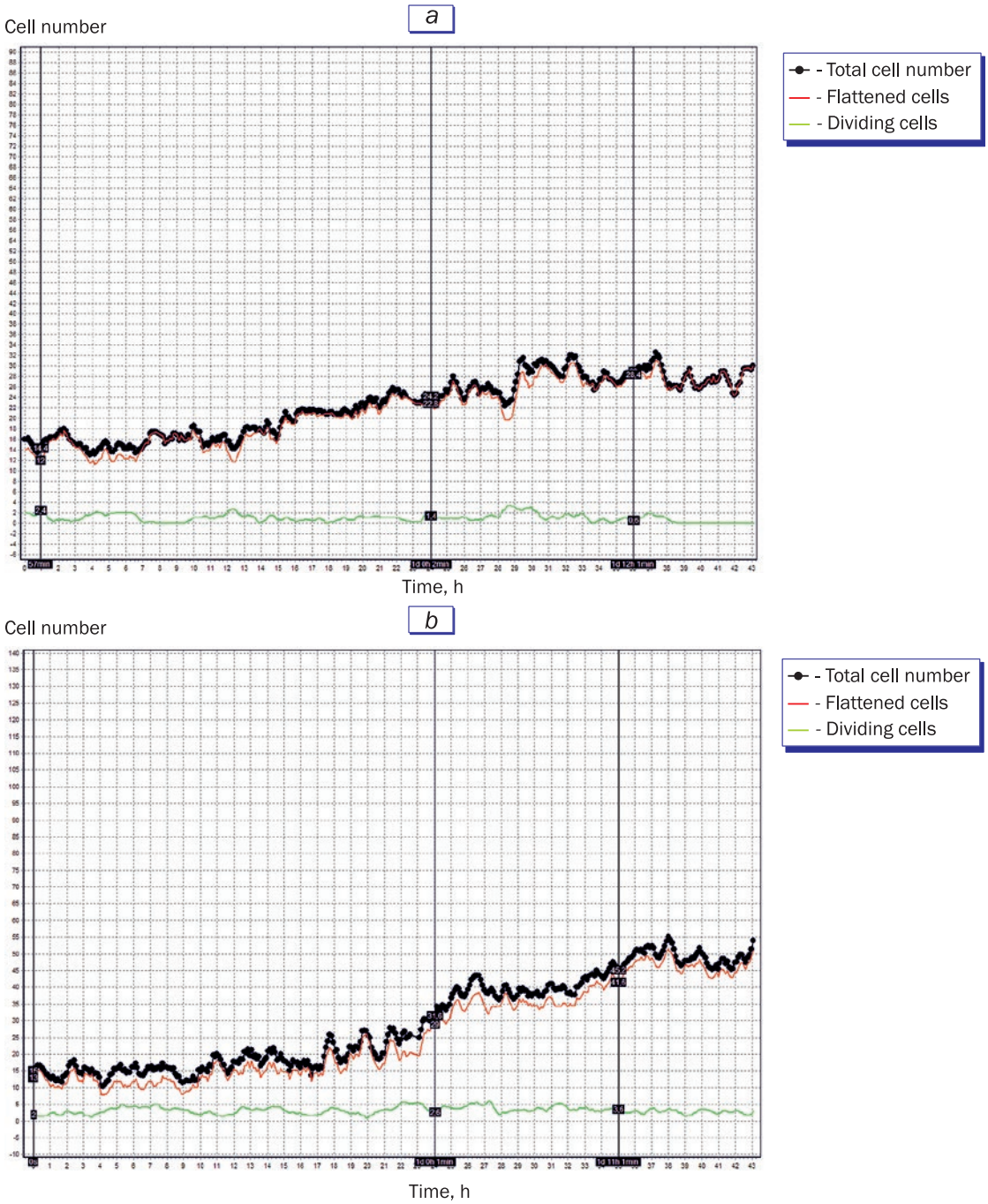

Fig. 5. Analysis of proliferative activity of primary porcine chondroblasts (*a*) and osteoblasts (*b*).

equipment was kindly provided by the Center Regenerative Medicine and Cell Technologies Common Use Centre organized on the basis of Innovative Medical Technology Center (Medical Technopark).

Analysis of proliferative capacity (mitotic index), trajectories of cell migration, and motor activity was performed with the support of the budget project No. 0324-2016-0003 Institute of Cytology and Genetics, Siberian Division of the Russian Academy of Science and analysis of cell mobility on substrates with different stiffness was supported by budget project No. 0324-2016-0008 of the Institute of Cytology and Genetics, Siberian Division of the Russian Academy of Science.

REFERENCES

1. Deev RV, Isaev AA, Tsupkina NV, Pinaev GP, Bozo IJ, Grebnev AR, Kaligin MS. The tissue engineering bone: a methodological basis and biological properties. Geny Kletki. 2011;6(1):62-67. Russian.

2. Komlev VS, Sergeeva NS, Fedotov AYu, Sviridova IK, Kirsanova VA, Akhmedova SA, Teterina AYu, Zobov YuV, Kuvshinova EA, Shanskii YaD, Barinov SM. Analysis of physicochemical and biological properties of composite alginate-calcium phosphate matrices intended for the use in prototyping technologies for replacement of bone defects Materialovedenie. 2016;(3):38-42. Russian.
3. Nashchekina YA, Nikonov PO, Mikhailov VM, Pinaev GP. Distribution of bone-marrow stromal cells in a 3D scaffold depending on the seeding method and the scaffold inside a surface modification. Cell Tissue Biol. 2014;8(4):313-320.
4. Cao X, Lin Y, Driscoll TP, Franco-Barraza J, Cukierman E, Mauck RL, Shenoy VB. A chemomechanical model of matrix and nuclear rigidity regulation of focal adhesion size. Biophys J. 2015;109(9):1807-1817.
5. De Santis R, Russo A, Gloria A, D'Amora U, Russo T, Panseri S, Sandri M, Tampieri A, Marcacci M, Dediu VA, Wilde C.J, Ambrosio L. Towards the design of 3D fiber-deposited poly(ε-caprolactone)/iron-doped hydroxyapatite nanocomposite magnetic scaffolds for bone regeneration. J. Biomed. Nanotechnol. 2015;11(7):1236-1246.
6. Di Silvio L, Gurav N. Osteoblasts. Human Cell Culture. Koller MR, Palsson BO, Masters JRW, eds. London, 2001. P. 221-241.
7. Dillon JP, Waring-Green VJ, Taylor AM, Wilson PJ, Birch M, Gartland A, Gallagher JA. Primary human osteoblast cultures. Methods Mol. Biol. 2012;816:3-18.
8. Hadjicharalambous C, Buyakov A, Buyakova S, Kulkov S, Chatzinikolaidou M. Porous alumina, zirconia and alumina/zirconia for bone repair: fabrication, mechanical and in vitro biological response. Biomed. Mater. 2015;10(2). ID 025012. doi: 10.1088/1748-6041/10/2/025012.
9. Hadjicharalambous C, Mygdali E, Prymak O, Buyakov A, Kulkov S, Chatzinikolaidou M. Proliferation and osteogenic response of MC3T3-E1 pre-osteoblastic cells on porous zirconia ceramics stabilized with magnesia or yttria. J. Biomed. Mater. Res. A. 2015;103(11):3612-3624.
10. Huang L, Cai X, Li H, Xie Q, Zhang M, Yang C. The effects of static pressure on chondrogenic and osteogenic differentiation in condylar chondrocytes from temporomandibular joint. Arch. Oral Biol .2015;60(4):622-630.
11. Iandolo D, Ravichandran A, Liu X, Wen F, Chan JK, Berggren M, Teoh SH, Simon DT. Development and characterization of organic electronic scaffolds for bone tissue engineering. Adv. Healthc. Mater. 2016;5(12):1505-1512.
12. Khang G. Intelligent Scaffolds for Tissue Engineering and Regenerative Medicine. Boca Raton, 2012. P. 589-606.
13. Maeda A, Bandow K, Kusuyama J, Kakimoto K, Ohnishi T, Miyawaki S, Matsuguchi T. Induction of CXCL2 and CCL2 by pressure force requires IL-1β-MyD88 axis in osteoblasts. Bone. 2015;74:76-82.
14. Pati F, Song TH, Rijal G, Jang J, Kim SW, Cho DW. Ornamenting 3D printed scaffolds with cell-laid extracellular matrix for bone tissue regeneration. Biomaterials. 2015;37:230-241.
15. Selmeczi D, Mosler S, Hagedorn PH, Larsen NB, Flyvbjerg H. Cell motility as persistent random motion: theories from experiments. Biophys. J. 2005;89(2):912-931.
16. Smith BD, Grande DA. The current state of scaffolds for musculoskeletal regenerative applications. Nat. Rev. Rheumatol. 2015;11(4):213-222.
17. Tsekov R, Lensen M. Brownian motion and temperament of living cells. Chin. Phys. Lett. 2013;30(7):ID 070501.
18. Tsiridis E, Gurav N, Bailey G, Sambrook R, Di Silvio L. A novel ex vivo culture system for studying bone repair. Injury. 2006;37(Suppl. 3):S10-S17.
19. Wang T, Yang X, Qi X, Jiang C. Osteoinduction and proliferation of bone-marrow stromal cells in three-dimensional poly(ε-caprolactone)/hydroxyapatite/collagen scaffolds. J. Transl Med. 2015;13:152. doi: 10.1186/s12967-015-0499-8.
20. Yin B, Ma P, Chen J, Wang H, Wu G, Li B, Li Q, Huang Z, Qiu G, Wu Z. Hybrid macro-porous titanium ornamented by degradable 3D Gel/nHA micro-scaffolds for bone tissue regeneration. Int. J. Mol. Sci. 2016;17(4):575. doi: 10.3390/ijms17040575.